A COMPARISON OF FINE AND COARSE RESOLUTION REMOTE SENSING PLATFORMS FOR POST FIRE SEVERITY

by

Maximilian E. Petri

A directed research report submitted to the Geography Department of
Texas State University in partial fulfillment
of the requirements for the degree of
Master of Applied Geography
with a specialization in Geographic Information Science

December 2019

Committee Members:

Dr. Nathan Currit

Dr. Yanan Nancy Li

TABLE OF CONTENTS

ACKNOWLEDGMENTS

I'd like to thank Austin Fire Department-Wildfire Division and Nate Casebeer; my advisors Dr. Nate Currit and Dr. Nancy Li; Planet for allowing me access to the required imagery and Sara Safavi; Dr. Jennifer Devine and the Research Design students; Dr. Edwin Chow and Rich Lee; Tray Duncan and the Nowlin family ranch; Scott, Jeff, and Carl at the Balcones National Wildlife Refuge; Tim Harten and the Llano Volunteer Fire Department; and most of all my wife and kids Jamey, Madeline, and Julianne.

This work is dedicated to the wildfire fighters and managers, who choose their profession and choose to go into danger.

LIST OF FIGURES

ABSTRACT

This study compares Landsat 8 dNBR with Planet dNDVI for burn severity measurement. The sensors were compared to ground reference data using the Composite Burn Index (CBI) and a radiospectrometer. CBI data was collected with 21 field plots from a fire on ranch land in Llano, Texas in the Summer of 2018. dNBR based on Landsat 8 produced higher r^2 values (0.742) than dNDVI based on Planet imagery (0.324). Planet imagery at ~3m spatial resolution has finer details of the landscape that can help land managers, fire departments, and landowners to rehabilitate the landscape, but it lacks an MIR band, which explains its lower correlation values. The Landsat system provides better results spectrally, but Planet images can provide finer detail of the landscape and with a more flexible time/date range.

Keywords: Burn Severity; Planet; Landsat; NBR; NDVI; Texas

INTRODUCTION

Wildfires are dangerous and destructive events that can affect a large amount of natural and human spaces. California has a high risk of wildfire hazard (Chou, Y. H., et al. 1990; Roy, D. R. et al. 2006; Corcoran, J. et al. 2007; Boer, M. M. et al. 2008; Cannon, S. H. et al. 2008; Miller, J. D. et al. 2009; Bradstock, R. A. et al. 2010); Texas has a growing risk of fires due to drought conditions and sub-urban sprawl (Nox, R. & Myles, C. C. 2017). Central Texas is located at the interface of woodland and shrubland, where vegetation can grow dense enough to fuel a wildfire, but drought conditions also routinely arise to provide a separate conducive environment for wildfires. To learn more about wildfire risk, fire departments conduct severity assessments after a wildfire to measure the total area burned and intensity of the burning. As part of the severity assessment and research, fire investigators conduct evaluations on the ground and aerial evaluations (using Landsat imagery) to measure and describe the impact of the fire. In central Texas, the existence of two catalytic environmental conditions (dense vegetation and drought conditions) presents a unique challenge to accurate and clear depiction of wildfire effects on the landscape.

This research aims to aid stakeholders in planning for restoration of land that has been impacted by wildfire. These stakeholders, including fire departments and emergency services, landowners, governmental leaders and the public at large, require the latest, exhaustive information about the extent and degree of a wildfire burn scar on the landscape to plan for remediation.

To measure wildfire scars, analysts depend on remote sensing methods and imagery; these calculations are critical for successful and cost-effective restoration activities. Yet, recent innovations in remotely sensed imagery have yet to be applied to wildfire scar assessments in

Central Texas despite the prevalence of fires. My research question is: How does fine spatial and temporal resolution multispectral imagery of latest technologies (Planet®) compare to widely used conventional hyperspectral coarse imagery (Landsat) in the measurement of wildfire severity in Central Texas? To answer this question, I draw on the case study of the wildfire in Llano, Texas during Summer 2018.

As remote sensing technologies have evolved, current techniques used to measure the severity of wildfires require ongoing study and assessment. The Dove platform by Planet® is the newest technology available in the area of satellite imagery. This service provides ~3 meter spatial resolution, 4 band spectral resolution (blue, green, red and near-infrared), and daily overhead revisit. The advantage of Planet imagery is its revisit period of 1 day. The spatial resolution is high, but not the highest in the industry. The spectral resolution is equal to other high resolution sensors, but less than coarser resolution sensors. In my study of wildfires in Central Texas, I hypothesize that the use of the finer spatial resolution provided by newer technologies (Planet) will provide a more statistically significant measurement of wildfire burn severity than research studies that utilize older technologies (Landsat).

LITERATURE REVIEW

The literature has been divided into bodies of literature: Applying the Normalized Burn Ratio Method to Calculate Wild-fire Severity with Landsat Imagery, Mechanisms of Wildfires, Remote Sensing of Wild-Fires, and Using Planet Imagery to Analyze Land Cover Change with NDVI. The sections on the Normalized Burn Ratio, remote sensing of wild-fires, and using NDVI Planet imagery support the methods for burn severity measurement, field methods, and comparing the sensors. The Mechanisms of Wildfires section supports the understanding of wildfires and interaction with the terrain.

Applying the Normalized Burn Ratio Method to Calculate Wild-fire Severity with Landsat Imagery

The importance of fire severity analysis is valuable information to forest services and fire departments globally. These stake holders need information about fire severity to: (1) document the effects of fires, (2) manage the restoration and recovery of the land, (3) update forest and grassland maps, (4) serve as reference data for future observation and research, and (5) evaluate management and policy implications (Brewer et. al., 2005). The authors discuss the use of the Normalized Burn Ratio (NBR) to assist in answering the above questions. Using Landsat TM imagery the authors used the equation (TM4 - TM7)/(TM4 + TM7); where TM4 is Landsat TM band 4 or near-infrared (NIR) and TM7 is Landsat TM band 7 or mid-infrared (MIR) wavelengths. This can also be applied to other multi-spectral imagery platforms as

$$\mathrm{NBR} = \frac{\mathrm{NIR} - \mathrm{MIR}}{\mathrm{NIR} + \mathrm{MIR}}$$

The authors extended their process by calculating a difference using the equation (TM4 – TM5)/(TM4 + TM5); where TM5 is a second mid-infrared (MIR) wavelength on Landsats 4 and

5 (Brewer et. al., 2005). Further, Brewer et al. use a principal components method to reduce the imagery data to burned and unburned terrain (Brewer et al., 2005).

Key and Benson (1999) gave a presentation of their initial findings for burn severity mapping of National Parks using remote sensing and the Normalized Burn Ratio for the first time to measure the burn severity of the fires. The authors used Landsat 5 and 7 imagery to map the changes. The initial assessment, immediately post-fire, showed that the burned area was well defined, but clouds, sun geometry, and dryness obscured some of the burn area. When they conducted an additional assessment the following growing season, the results were better and still showed the burned area. Key and Benson also described the impacts of fire on the terrain. Due to the ecological changes caused by wildfire, landowners (whether public or private) need fire severity assessments to recover and remediate the landscape. Wildfires will impact the surface landscape (clearing vegetation) but can also destabilize the soil beneath. Following a wildfire, scorched soil can become prone to erosion because of the eradication of root systems that once held soil in place. In the event of heavy rains following a wildfire event, this can cause additional hazardous conditions like flooding. This presentation caused an operationalization of the NBR for land managers and fire managers (Key & Benson, 1999).

Key et al. (2006), produced the USDA technical journal now widely cited and used by fire managers globally, the FIREMON: Fire and effects monitoring and inventory system. Key et al. (2006), define burn severity and discuss the tools for measuring it. The authors describe the process for Composite Burn Index (CBI) which is the ground reference data or field data, created by fire management teams. The CBI can then be used to see if it correlates with remotely sensed NBR datasets and other variants. I used the FIREMON journal to support field data collection (Key et al., 2006). Further, newer imagery of this area can be compared to Landsat imagery to

provide “quantitative continuous change image[s] linked directly to actual quantitative change[s] in vegetation condition” (Brewer et. al., 2005).

Boer et al. (2008) expand upon the NBR equation to include a temporal difference. They create the delta normalized burn ratio (ΔNBR), which quantifies burn severity based on the pre-fire and post-fire NBR conditions. Where the equation,

$$\Delta NBR = NBR_{pre\text{-}fire} - NBR_{post\text{-}fire}$$

is used to calculate a differenced image from the pre-fire and post-fire imagery. Further, the ΔNBR was calibrated against ground reference data and satellite imagery from Leaf Area Index (LAI) measurements. The goal of their study was to compare the measurements of LAI and ΔNBR. The authors conducted their research across southern Australia, where LAI was predicted by models using NBR or the Normalized Difference Vegetation Index as variables. Next, they applied the models using temporal differences. Boer et al. found that ΔNBR and ΔLAI were strongly related with each other at 85% on a linear regression. Further, the authors found that ΔLAI was better at predicting a location of fire-severity than ΔNBR. However, the authors admit that the photographic LAI method only measured the overstory or canopy of a forest and not the understory. In cases of wild-fire, the understory is the most abundant fuel for the fire and needs to be measured (Boer et al., 2008).

Mechanisms of Wildfires

Bradstock et al. (2010) studied the effects of weather, fuel, and terrain on fire severity across the Australian landscape using linear regression. Fire-severity was the dependent variable and weather (categorized as extreme or not extreme), TOPOS (the Euclidean distance to the nearest high ground), slope, aspect (categorized as north, south, east, or west), and time-since-fire (number of years) were the independent variables. The authors found weather was the

dominating factor influencing fire-severity. Further, they found that overstory fires were more likely on ridges, (exposure to wind, less humidity) and less likely on valley bottoms, (less wind, more humidity) (Bradstock et al., 2010).

Remote Sensing of Wild-Fires

Kokaly et al. (2007) studied the differences between hyper-spectral and multi-spectral sensors to map the characteristics of surface materials. Similar to van Wagtendonk et al.(2004), Kokaly et al. (2007) examined AVIRIS and ETM+ images compared to CBI reports, but they also focused on the changes to soil. The purpose of their study was to examine how change in soil can affect erosion after the fire. They concluded "[in] areas greatly heated by the fire, soil structure can be destroyed and water infiltration rates reduced, producing rapid runoff and hillslope erosion." (cited in Kokaly et al., 2007.) The authors concluded that ETM+ was successful at detecting burn severity at 81% overall accuracy and 0.55 kappa statistic. However, ETM+ overestimated scorched trees and ash/char compared to the AVIRIS platform (Kokaly et al., 2007).

Kolden et al. (2012) conducted research on the segments of forests that were not burned in a wildfire and how this could skew total burned area. The researchers applied the ΔNBR to examine the burned extent in Glacier NP, Yosemite NP, and Yukon-Charley Rivers NP in the Western US. Within the fire perimeters, Yosemite had 37%, Glacier had 17%, and Yukon-Charley had 14% area that was classified as unburned. Kolden et al. focus their study area on national parks and forests, leaving out shrub-land and grass-land. The authors state that "area burned, is one of the most inconsistently recorded metrics of wildfire activity and one of the least accurate across datasets and studies," (Kolden et al., 2012). Further, the extent and shape of the unburned areas within the fire perimeter are key characteristics of wildfires that have not been

described by most of the literature on the subject. The authors describe that coarser spatial resolution (250m to 1000m) in imagery, i.e. the Moderate Resolution Imaging Spectroradiometer (MODIS) imagery, can erroneously estimate 72% of burned area. Additionally, unburned areas can be an indicator of places of refuge for the fauna of the forest; and thereby a starting point for post-fire recovery of vegetation and wildlife. The authors conclude that there was a significant negative relationship between regressed burn severity and unburned parts, meaning larger fires would have smaller unburned shares; conversely, their data in the national parks displayed weak relationships between burn severity and unburned areas. Additional research must be completed to confirm the relationships (Kolden et al., 2012). This piece is important to my research because it exemplifies the use of higher resolution sensors over moderate resolution sensors to quantify the size of a burned area .

van Wagtendonk et al. (2004) compared the usage of Airborne Visible and Infrared Spectrometer (AVIRIS) imagery with Landsat 7 Enhanced Thematic Mapper Plus (ETM+) imagery for applications to measuring burn severity. The key differences characteristics in the platforms for AVIRIS to ETM+ are airborne vs. satellite; contiguous hyper-spectral vs. multi-spectral; and higher spatial resolution at 17m vs. 30m spatial resolution respectively. Another key difference is the complexity of an AVIRIS mission. This type of mission is conducted by plane. Therefore, the temporal resolution of AVIRIS is per mission tasked, while ETM+ is constant at 16 day intervals. Further, this mission planning has a high monetary cost to operate. The authors confirmed that the AVIRIS channels 47 and 210 correctly measured the similar measurements for bands 4 and 7, NIR and MIR respectively. This was also correlated with CBI measurements, $r^2 = 0.894$ for ETM+ and $r^2 = 0.853$ for AVIRIS. The authors found that AVIRIS

had similar results to measure burn severity as ETM+; however, at a much higher cost and operational planning requirement (van Wagtendonk et al., 2004).

Using Planet Imagery to Analyze Land Cover Change with NDVI

Houborg and McCabe (2016) describe an early assessment of the Planet constellation of satellites, which at the time of writing were still only RGB image and lacked the NIR band of the current fleet and global daily coverage. The authors used methods to augment Landsat 8 NDVI imagery using the visible bands of Planet and as well as MODIS imagery using rule-based decision tree regression models. Houborg and McCabe designed a model that translated Planet RGB into atmospherically corrected Landsat 8. Their study area was on center-pivot agricultural plots in Saudi Arabia. They tested the hypothesis and achieved highest correlations of accuracy when Planet and Landsat acquisition dates were as close as possible. MODIS imagery was used in this process as a backstop to correct differences between Landsat 8 and Planet. The workflow included a multi-variate regression model to render Planet RGB to Landsat NDVI. The cubist approach was used to create the models and resulting regressions (Houborg & McCabe, 2016).

Helman et al. (2018) compared Planet imagery of four different vegetation indices to in-situ assessments of vine stem water content, specifically to aid in vineyard efficiency and estimate the moisture content in large sections of the vine stem of vineyards in Israel. The authors analyzed the vineyard landscape with Enhanced Vegetation Index, Soil-Adjusted Vegetation Index, Green NDVI, and NDVI to compare it to onsite vine stem water content. They tested the vegetation indices for predicting weekly stem moisture on a single vineyard using: (1) multivariable linear model against the vegetation indices, (2) single linear regression to test for whole season stem moisture, and (3) a global multivariate linear model again using the weekly vegetation indices, but with an expanded population across 81 vineyards. The authors concluded

that the Soil-Adjusted Vegetation Index had the best results in predicting stem moisture content (Helman et al., 2018). The research conducted by Helman et al., 2018 draws on current studies that use NDVI to measure vegetation change.

I will contribute to the bodies of literature by comparing Planet imagery NDVI analysis to Landsat 8 NBR images for burn severity purposes. Further, I tested both NDVI and NBR against ground-reference data collected from CBI surveys. To analyze the images in both methods, correlation will be used to test the hypothesis. Similar to van Wagtendonk et al., (2004), I will compare method A (Landsat8) to method B (Planet) using Pearson's R correlation.

METHODOLOGY

Study Area

The case I will use to test the utility of Planet imagery for burn severity is near Llano, TX off TX Highway 71 on ranch properties where a fire occurred on 19 July 2018 (Figure 1). The fire burned for 3 days, and burned a little over 1000 acres.

Located in the Edwards Plateau, the terrain consists of rolling hills, with shrubby to woodland vegetation. The Llano Basin, that contains Llano County, consists of granite and sandy soils. The rocky soils support tall and mid-grasses, yucca (*Yucca spp.*), and live oak (*Quercus virginiana*), ashe juniper (*Juniperus ashei*), and mesquite (*Prosopis glandulosa*) trees. Adjacent clay soils will support bluestems, gramas, indiangrass, buffalograss, witchgrass, lovegrass, and Texas wintergrass (Texas State Historical Association).

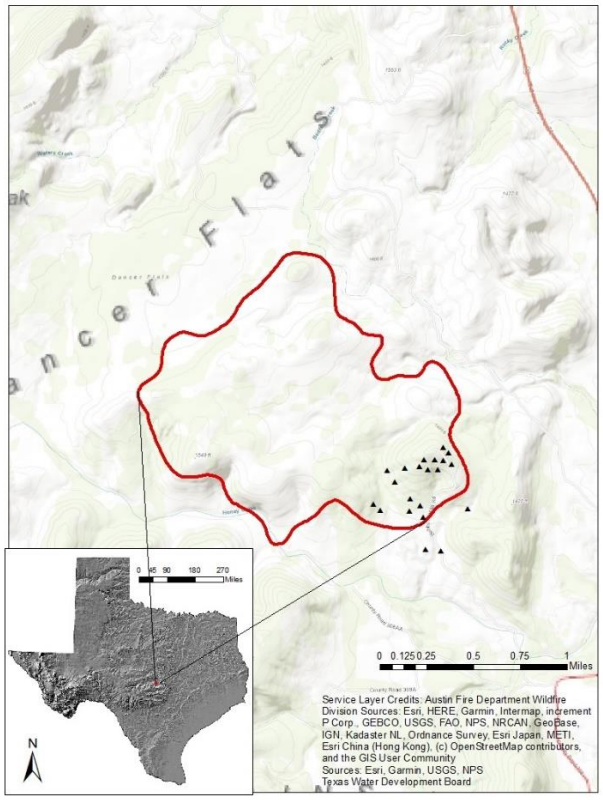

Fig. 1: Study Area of Llano Highway 71 Wildfire with plot locations.

The study area centers around the southeastern quadrant of the fire, where the fire originated. The landowners described that the fire was not the first fire on the property, but the first this large and first known in that location. A few years before the fire, the property had been cleared of almost all of the ashe juniper trees to allow for cattle grazing. When the fire took place, strong northwestern winds fanned the flames and carried the fire to the remaining properties within the affected fire perimeter. In some cases, the fire jumped roads and came close to burning the landowner's house, but fortunately circumvented the house. The Llano Volunteer Fire Department, supported by the Austin Fire Department, responded to the fire and worked to contain and save property for three days, including the use of helicopter fire suppression.

Data

In my research, I made in-situ excursions to survey a previously burned area including the central Texas wildfire in Llano (19–21 July 2018). Ground reference data was acquired using the Composite Burn Index method of collection. CBI data was collected using the FIREMON Form, see Appendix, collecting at ~20 plots and 30 meter plots. The locations are selected within a stratified sampling area. CBI data was collected one year post-fire from August, 22 2019 to September, 26 2019, among 21 plots, three of them unburnt calibration plots outside of the burn perimeter. The 30m CBI plots were centered around the southeastern ranch at the point of origin of the fire. Plot 11 (Figure 2) had the highest burn investigated and was on the northeastern facing slope, northeast of the ranch house. Plot 17 (Figure 3) was of interest because of its proximity to the neighboring ranch where ashe junipers were not cleared and exhibited moderate burn severity compared to high severity in the neighboring property.

Fig. 2: Plot 11, highest burn severity examined.

Fig. 3: Plot 17, moderate burn severity examined, in the background readers can observe the property line where there was uncleared ashe juniper and higher severity burn.

In-situ data collection also consisted of radiospectrometer-based reflectance data, using the Advanced Spectral Devices (ASD) device. The center of the 30m CBI plots were used and were collected in a 3m bounding square around the center. The reflectance data was collected on sunny/almost cloudless skies on August 29, 2019 and September 19 and 26, 2019. Eight scans were taken and then averaged in post-processing to create a 3 meter data value. The sun was on the author's back and holding the pistol grip attachment at approximately 1.25m above target. See Appendix for example plot form.

Analytical Methods

The methods used to investigate the satellite imagery include quantitative analysis and the Normalized Burn Ratio ie. (NIR - MIR)/(NIR + MIR) and dNBR ie. $NBR_{pre\text{-}fire} - NBR_{post\text{-}fire}$ to measure burn severity. I compare Landsat 8 (Method A) imagery with Planet (Method B) imagery. I quantitatively measure the differences between methods using Pearson's correlation coefficient. Specifically, output pixels between each dataset will be compared for correlation. Datasets include Landsat imagery, Planet imagery, a field gathered Composite Burn Index, and local fire department data from Austin FD and Llano VFD.

For method A, Landsat data was downloaded from the USGS EarthExplorer website and used for analysis pre-fire (July 3, 2018), immediately after the fire (August 20, 2018), and one year after the fire (July 6, 2019); to reiterate the fire occurred July 19-21, 2018. The imagery used will be Landsat 8 level 2 images corrected for surface reflectance, bands 5 (NIR) and 7 (SWIR 2) with 30 meter spatial resolution and 16-bit radiometric resolution. The imagery was processed and analyzed with ERDAS Imagine desktop application computing the NBR and dNBR equations of the images.

For method B, Planet data was downloaded from the Planet Explorer website and used for analysis pre-fire (July 3, 2018), immediately after the fire (August 20, 2018), and one year after the fire (July 6, 2019). The imagery used was PlanetScope surface reflectance, bands 3 (Red) and 4 (NIR) at 3 meter spatial resolution and 16-bit radiometric resolution. The imagery was processed with ERDAS for computing the NDVI and dNDVI to compare with method A. To equalize the comparison between 3m spatial resolution and 30m resolution, the Planet images were resampled to 30m. Method A and Method B were analyzed as independent variables to the dependent variable ground reference data of the CBI using Pearson's correlation coefficient.

RESULTS AND DISCUSSION

The burn-severity was examined using by comparing dNBR and dNDVI. The first cloud free pre-fire and post-fire images of the study area occurred on July, 3 2018 and August, 20 2018. dNBR Landsat 8 produced higher r^2 values (0.742) than dNDVI based on Planet imagery (0.324), both at the 95% confidence interval (Figure 4). dNBR on Landsat 8 had more than double the correlation values of Planet most likely because of the use of the MIR band. Further, the positive linear relationship is because the higher positive dNBR and dNDVI values displayed higher burn severity, while lower positive values (closer to zero) were the less burnt and unburnt plot values.

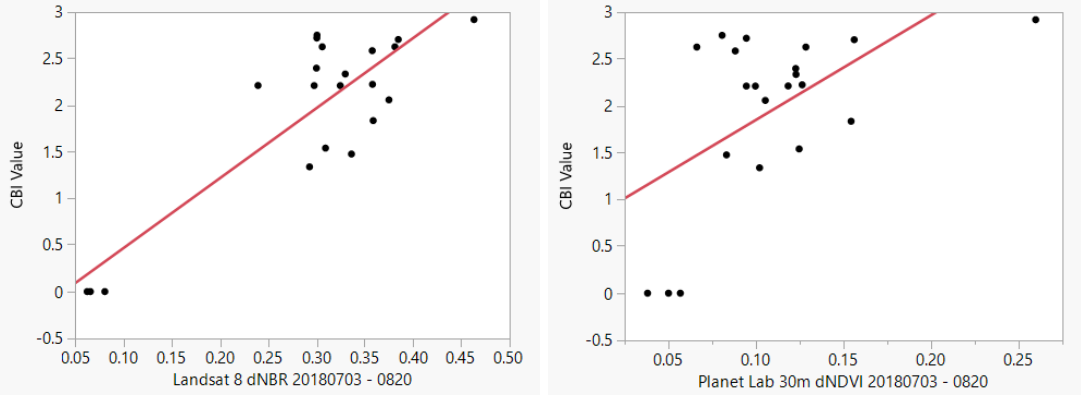

Fig. 4: Landsat 8 (left) dNBR Pre-fire 20180703 to Post-fire 20180820 displayed against CBI $r^2 = 0.742$, and Planet 30m (right) dNDVI Pre-fire 20180703 to Post-fire 20180820 displayed against CBI $r^2 = 0.324$.

The images were also compared for single date normalized burn ratio measurements using August, 20 2018. The images from NBR Landsat 8 and NDVI Planet sensors produced similar clusters in comparison to the dependent CBI values. NBR Landsat 8 produced higher r^2 values (0.696) than NDVI based on Planet r^2 (0.342), both at the 95% confidence interval (Figure 5). Again, NBR on Landsat demonstrated the higher correlation values than NDVI on Planet because of the use of the MIR band. Further, this comparison may not be the most suitable, as the NBR and NDVI do not measure severity, while CBI does measure the severity.

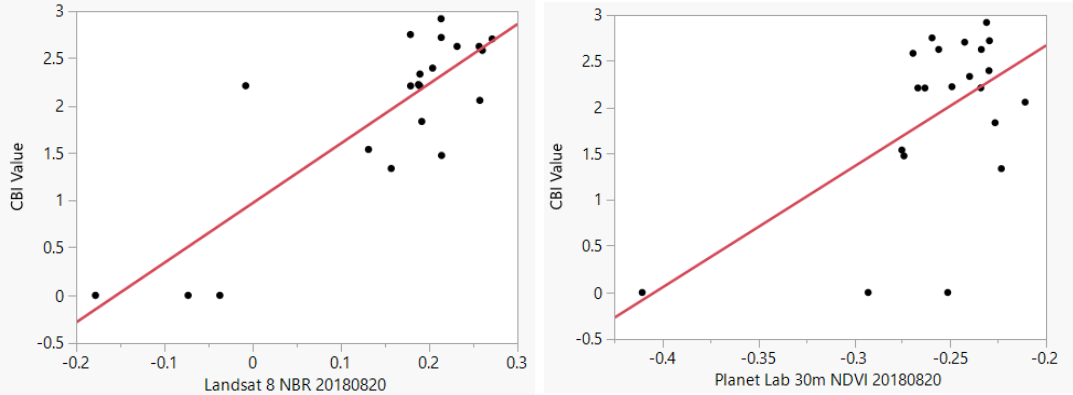

Fig. 5: Landsat 8 (left) NBR Post-fire 20180820 displayed against CBI r^2 = 0.696, and Planet 30m (right) NDVI Post-fire 20180820 displayed against CBI r^2 = 0.342.

Using pre-fire image date of July, 3 2018 and post-fire date of July, 6 2019, the Landsat 8 and Planet images were compared to the dependent CBI. For this comparison both sensors had low correlation with CBI. Landsat 8 had lower r^2 values (0.104) than Planet (0.149), again at the 95% confidence interval (Figure 6). This was most likely because of the inherent study area landscape of grasses and shrubs that had rebounded post-fire, one year later (including the growing season), and displayed higher photosynthetic vegetation reflectance and regrowth, no longer showing signs of the burn.

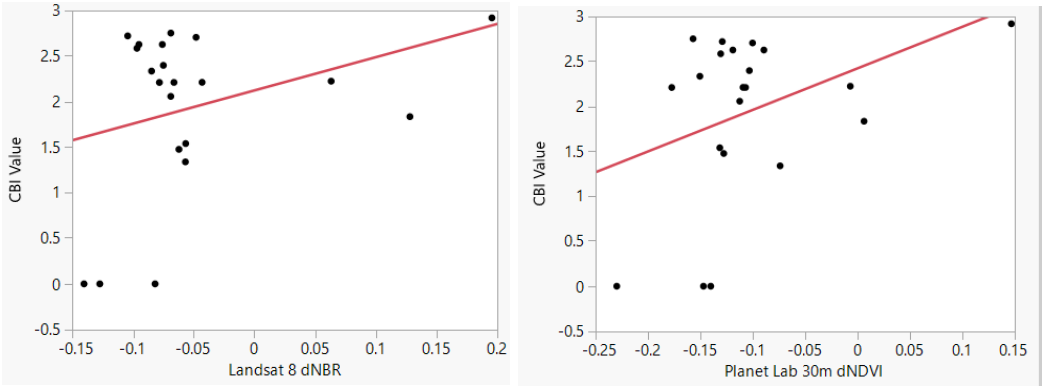

Fig. 6: Landsat 8 (left) dNBR Pre-fire 20180703 to Post-fire 20190706 displayed against CBI r^2 = 0.104, and Planet 30m (right) dNDVI Pre-fire 20180703 to Post-fire 20190706 displayed against CBI r^2 = 0.149.

The actual dNBR and dNDVI images produced by Landsat 8 and Planet for July, 3 2018 and August, 20 2018 had interesting results. The Landsat dNBR imagery showed similar levels in burn where they were observed during the in-situ CBI. Planet dNDVI imagery also displayed sufficient results for classifying burn severity; however, the Planet dNDVI image would need masking out the unburned perimeter around the fire as the dNDVI was not capable of differing unburnt from burnt terrain, where Landsat dNBR was capable (Figure 7).

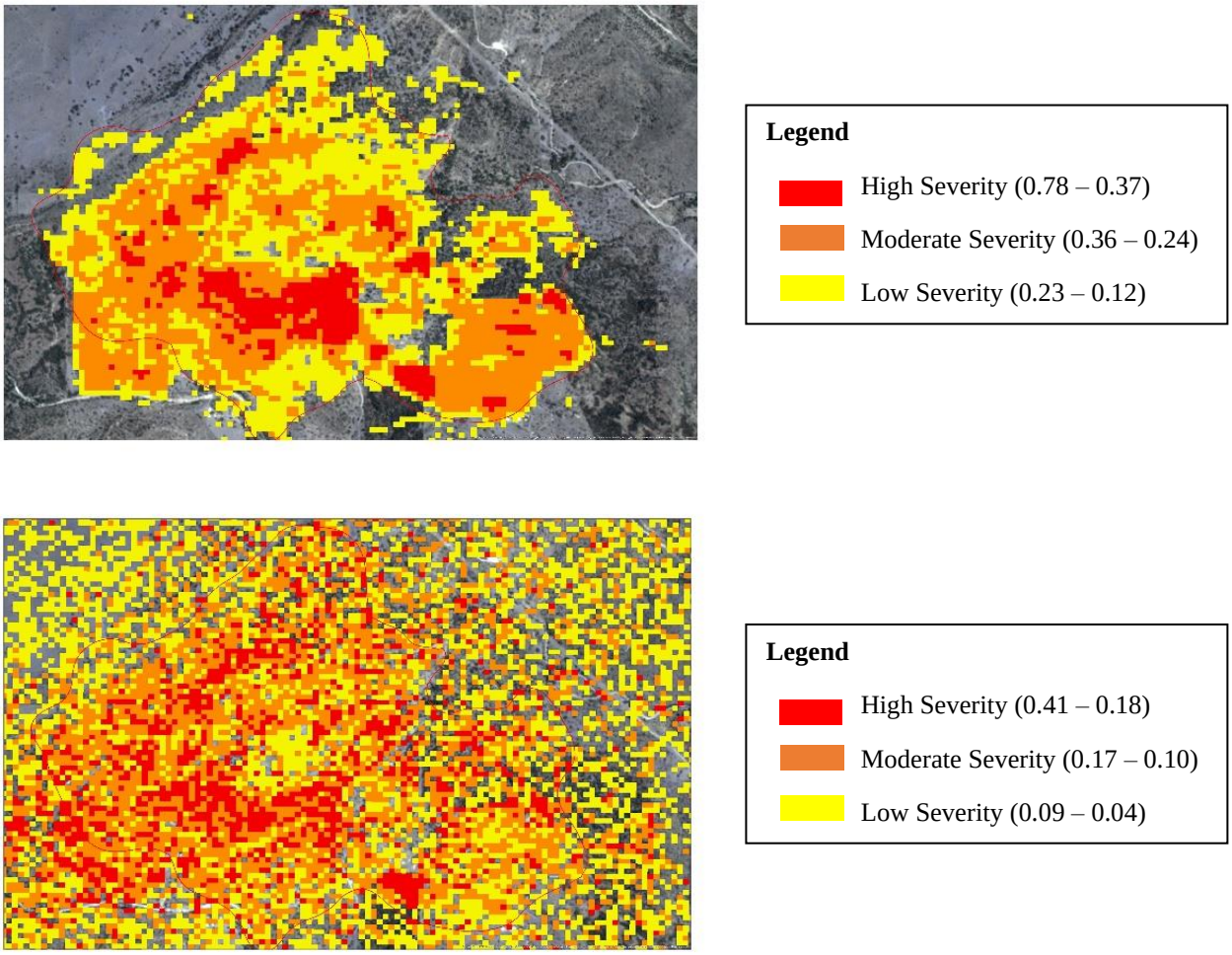

Fig. 7: Landsat 8 dNBR (left) Planet dNDVI (right) at the same scale and extent, Planet dNDVI overclassified across all severities, but mostly overclassifed in low severity burn.

Radiospectrometer data was collected for all of the plots. Of interest, Planet reflectance had higher values than in-situ data from the radiospectrometer, except in the plot 13 case visible below where the NIR band reflectance was lower than radiospectrometer data (Figure 8).

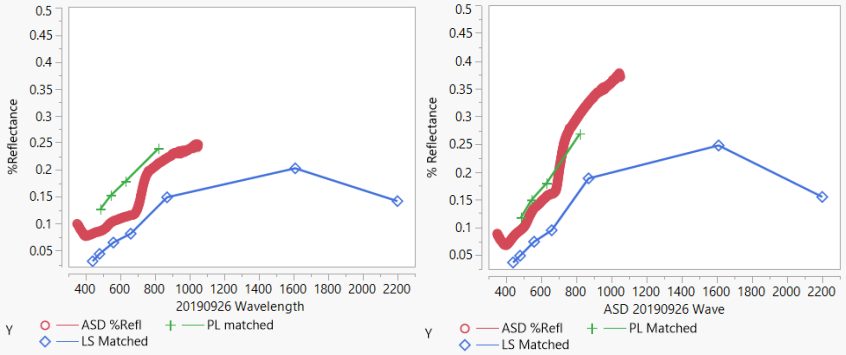

Fig. 8: Reflectance graph of ASD radiospectrometer, Planet, and Landsat8. (Left) Plot 11, highest burn severity. (Right) Plot 13, calibration plot, no burn.

CONCLUSIONS

To reiterate, this research compares the imagery sources of Landsat to Planet as used in burn severity measurement in Central Texas. Ideally, Planet imagery has finer details of the landscape that can help land managers, fire departments, and landowners to rehabilitate the landscape. However, spectrally, Planet lacked an MIR band, which explains the higher correlation values of Landsat. Of each date example, the differenced index immediately after the fire (7/3/2018 - 8/20/2018) produced highest correlation values; and differencing a year later (7/3/2018 – 7/6/2019) was the only example where Planet had higher correlation values than Landsat, albeit both had insignificant r^2 values. My intent is to aid stakeholders in planning for restoration of land that has been impacted by wildfire, that will reduce frustration because of future wildfire susceptibility, soil degradation, and runoff creation. Planet, the company, plans to send more sensor assets into orbit including sensors called “SuperDoves” that would have more spectral options, including MIR, and even finer spatial resolution. Future research can be devoted to other regions (California, the Rockies, Australia) and landscapes, especially ones with larger tree populations. Further, principal components analysis and trying other indices with Planet imagery could help reveal more robust methods for burn-severity measurement and regrowth modeling.

REFERENCES

Boer, M. M., C. Macfarlane, J. Norris, R. J. Sadler, J. Wallace, and P. F. Grierson. 2008. Mapping burned areas and burn severity patterns in SW Australian eucalypt forest using remotely-sensed changes in leaf area index. *Remote Sensing of Environment* 112 (12):4358-4369.

Bohlin, I., H. Olsson, J. Bohlin, and A. Granstrom. 2017. Quantifying post-fire fallen trees using multi-temporal LiDAR. *International Journal of Applied Earth Observation and Geoinformation* 63:186-195.

Bradstock, R. A., K. A. Hammill, L. Collins, and O. Price. 2010. Effects of weather, fuel and terrain on fire severity in topographically diverse landscapes of south-eastern Australia. *Landscape Ecology* 25 (4):607-619.

Brewer, C. K., J. C. Winne, R. L. Redmond, D. W. Opitz, and M. V. Mangrich. 2005. Classifying and mapping wildfire severity: A comparison of methods. *Photogrammetric Engineering and Remote Sensing* 71 (11):1311-1320.

Cannon, S. H., et al. (2008). "Storm rainfall conditions for floods and debris flows from recently burned areas in southwestern Colorado and southern California." Geomorphology 96(3-4): 250-269.

Chou, Y. H., et al. (1990). "SPATIAL AUTOCORRELATION OF WILDFIRE DISTRIBUTION IN THE IDYLLWILD QUADRANGLE, SAN-JACINTO MOUNTAIN, CALIFORNIA." Photogrammetric Engineering and Remote Sensing 56(11): 1507-1513.

Corcoran, J., et al. (2007). "The use of spatial analytical techniques to explore patterns of fire incidence: A South Wales case study." Computers Environment and Urban Systems 31(6): 623-647.

Demšar, U., P. Harris, C. Brunsdon, A. S. Fotheringham, and S. McLoone. 2013. Principal Component Analysis on Spatial Data: An Overview. *Annals of the Association of American Geographers* 103 (1):106-128.

Helman, D., et al. (2018). Using Time Series of High-Resolution Planet Satellite Images to Monitor Grapevine Stem Water Potential in Commercial Vineyards. 10.

Henry, M. C. (2008). Comparison of single- and multi-date landsat data for mapping wildfire scars in Ocala National Forest, Florida. Photogrammetric Engineering and Remote Sensing 74 (7):881-891.

Houborg, R. and M. F. McCabe (2016). High-Resolution NDVI from Planet's Constellation of Earth Observing Nano-Satellites: A New Data Source for Precision Agriculture. 8.

Key, C. H., Z. Zhu, D. Ohlen, S. Howard, R. McKinley, and N. Benson, . , , . (2002). The normalized burn ratio and relationships to burn severity: Ecology, remote sensing and

implementation, Rapid Delivery of Remote Sensing Products. Paper read at Proceedings of the Ninth Forest Service Remote Sensing Conference (Jerry Dean Greer, editor), American Society for Photogrammetry and Remote Sensing, unpaginated CD-ROM.

Key, C. H., & Benson, N. C. InD. C. Lutes, R. E. Keane, J. F. Caratti, C. H. Key, N. C. Benson, S. Sutherland, & L. J. Gangi (Eds.), . (2006). Landscape assessment (LA). FIREMON: Fire effects monitoring and inventory system. , ed. F. S. U.S. Department of Agriculture, Rocky Mountain Research Station., (pp. LA−1–55). Fort Collins, CO.

Key, C. H., and Benson, N. C. (1999). Measuring and remote sensing of burn severity: the CBI and NBR. Poster abstract. In L. F. Neuenschwander and K. C. Ryan (Eds.), *Proceedings Joint Fire Science Conference and Workshop,* Vol. II, Boise, ID, 15-17 June 1999. University of Idaho and International Association of Wildland Fire. 284 pp. See http://jfsp.nifc.gov/conferenceproc/index.htm

Kokaly, R. F., B. W. Rockwell, S. L. Haire, and T. V. V. King. 2007. Characterization of post-fire surface cover, soils, and burn severity at the Cerro Grande Fire, New Mexico, using hyperspectral and multispectral remote sensing. Remote Sensing of Environment 106 (3):305-325.

Kolden, C. A., J. A. Lutz, C. H. Key, J. T. Kane, and J. W. van Wagtendonk. 2012. Mapped versus actual burned area within wildfire perimeters: Characterizing the unburned. *Forest Ecology and Management* 286:38-47.

Lentile, L. B., A. M. S. Smith, A. T. Hudak, P. Morgan, M. J. Bobbitt, S. A. Lewis, and P. R. Robichaud. 2009. Remote sensing for prediction of 1-year post-fire ecosystem condition. International Journal of Wildland Fire 18 (5):594-608.

Miller, J. D., and A. E. Thode. 2007. Quantifying burn severity in a heterogeneous landscape with a relative version of the delta Normalized Burn Ratio (dNBR). Remote Sensing of Environment 109 (1):66-80.

Miller, J. D., et al. (2009). "Calibration and validation of the relative differenced Normalized Burn Ratio (RdNBR) to three measures of fire severity in the Sierra Nevada and Klamath Mountains, California, USA." Remote Sensing of Environment 113(3): 645-656.

Nox, R. and C. C. Myles (2017). "Wildfire mitigation behavior on single family residential properties near Balcones Canyonlands Preserve wildlands in Austin, Texas." Applied Geography 87: 222-233.

Parks, S. A., G. K. Dillon, and C. Miller. 2014. A New Metric for Quantifying Burn Severity: The Relativized Burn Ratio. *Remote Sensing* 6 (3):1827-1844.

Roy, D. R., et al. (2006). "Remote sensing of fire severity: Assesing the performance of the normalized Burn ratio." IEEE Geoscience and Remote Sensing Letters 3(1): 112-116.

Texas State Historical Association (2017, 2017-11-19T00:00:00Z). "Texas Plant Life | Texas Almanac." from https://texasalmanac.com/topics/environment/texas-plant-life.

van Wagtendonk, J. W., R. R. Root, and C. H. Key. 2004. Comparison of AVIRIS and Landsat ETM+ detection capabilities for burn severity. Remote Sensing of Environment 92 (3):397-408.

Veraverbeke, S., S. Hook, and G. Hulley. 2012. An alternative spectral index for rapid fire severity assessments. Remote Sensing of Environment 123:72-80.

Planet imagery courtesy of Planet Labs, Inc.

Landsat imagery courtesy of USGS EarthExplorer.

APPENDIX

FIREMON LA Form

BURN SEVERITY – COMPOSITE BURN INDEX (BI)

PD - Abridged	Examiners:			Fire Name:		
Registration Code		Project Code		Plot Number		
Field Date mmddyyyy	/ /	Fire Date mmyyyy	/			
Plot Aspect		Plot % Slope		UTM Zone		
Plot Diameter Overstory		UTM E plot center		GPS Datum		
Plot Diameter Understory		UTM N plot center		GPS Error (m)		
Number of Plot Photos		Plot Photo IDs				

BI – Long Form	% Burned 100 feet (30 m) diameter from center of plot =							Fuel Photo Series =
STRATA RATING FACTORS	BURN SEVERITY SCALE							FACTOR SCORES
	No Effect	Low		Moderate		High		
	0.0	0.5	1.0	1.5	2.0	2.5	3.0	
A. SUBSTRATES								
% Pre-Fire Cover: Litter =	**Duff =**		**Soil/Rock =**	**Pre-Fire Depth (inches): Litter =**		**Duff =**	**Fuel Bed =**	Σ =
Litter/Light Fuel Consumed	Unchanged	–	50% litter	–	100% litter	>80% light fuel	98% Light Fuel	
Duff	Unchanged	–	Light char	–	50% loss deep char	--	Consumed	N =
Medium Fuel, 3-8 in.	Unchanged	–	20% consumed	–	40% consumed	--	>60% loss, deep ch	
Heavy Fuel, > 8 in.	Unchanged	–	10% loss	–	25% loss, deep char	--	>40% loss, deep ch	$\bar{X}$ =
Soil & Rock Cover/Color	Unchanged	–	10% change	–	40% change	--	>80% change	
B. HERBS, LOW SHRUBS AND TREES LESS THAN 3 FEET (1 METER):								
Pre-Fire Cover =			**% Enhanced Growth =**					Σ =
% Foliage Altered (blk-brn)	Unchanged	–	30%	–	80%	95%	100% + branch loss	
Frequency % Living	100%	–	90%	–	50%	< 20%	None	N =
Colonizers	Unchanged	–	Low	–	Moderate	High-Low	Low to None	
Spp. Comp. - Rel. Abund.	Unchanged	–	Little change	–	Moderate change	–	High change	$\bar{X}$ =
C. TALL SHRUBS AND TREES 3 to 16 FEET (1 TO 5 METERS):								
Pre-Fire Cover =			**% Enhanced Growth =**					Σ =
% Foliage Altered (blk-brn)	0%	–	20%	–	60-90%	> 95%	Signifcnt branch loss	
Frequency % Living	100%	–	90%	–	30%	< 15%	< 1%	N =
% Change in Cover	Unchanged	–	15%	–	70%	90%	100%	
Spp. Comp. - Rel. Abund.	Unchanged	–	Little change	–	Moderate change	–	High Change	$\bar{X}$ =
D. INTERMEDIATE TREES (SUBCANOPY, POLE-SIZED TREES)								
Pre-Fire % Cover =	**Pre-Fire Number Living =**				**Pre-Fire Number Dead =**			Σ =
% Green (Unaltered)	100%	–	80%	–	40%	< 10%	None	
% Black (Torch)	None	–	5-20%	–	60%	> 85%	100% + branch loss	N =
% Brown (Scorch/Girdle)	None	–	5-20%	–	40-80%	< 40 or > 80%	None due to torch	
% Canopy Mortality	None	–	15%	–	60%	80%	%100	$\bar{X}$ =
Char Height	None	–	1.5 m	–	2.8 m	–	> 5 m	
Post Fire: %Girdled =			**%Felled =**		**%Tree Mortality =**			
E. BIG TREES (UPPER CANOPY, DOMINANT, CODOMNANT TREES)								
Pre-Fire % Cover =	**Pre-Fire Number Living =**				**Pre-Fire Number Dead =**			Σ =
% Green (Unaltered)	100%	–	95%	–	50%	< 10%	None	
% Black (Torch)	None	–	5-10%	–	50%	> 80%	100% + branch loss	N =
% Brown (Scorch/Girdle)	None	–	5-10%	–	30-70%	< 30 or > 70%	None due to torch	
% Canopy Mortality	None	–	10%	–	50%	70%	%100	$\bar{X}$ =
Char Height	None	–	1.8 m	–	4 m	–	> 7 m	
Post Fire: %Girdled =			**%Felled =**		**%Tree Mortality =**			

Community Notes/Comments:	CBI = Sum of Scores / N Rated:	Sum of Scores	N Rated	CBI
	Understory (A+B+C)			
	Overstory (D+E)			
	Total Plot (A+B+C+D+E)			

% Estimators: **20 m Plot:** 314 m² 1% = 1x3 m 5% = 3x5 m 10% = 5x6 m
30 m Plot: 707 m² 1% = 1x7 m (<2x4 m) 5% = 5x7 m 10% = 7x10 m

After, Key and Benson 1999, USGS NRMSC, Glacier Field Station.
Version 4.0 8 27, 2004

Strata and Factors are defined in FIREMON Landscape Assessment, Chapter2, and on accompanying BI "cheatsheet." www.fire.org/firemon/lichtm

FIELD SPECTROMETER DATA

Project Name 308 Date/Time / 1013

Site ID/Photo Reference / Observer

GPS Grid Coordinates X: Y:

Instrument ID Number of Scans Averaged

Geometry of observer's position relative to incident radiation: (sketch or description)

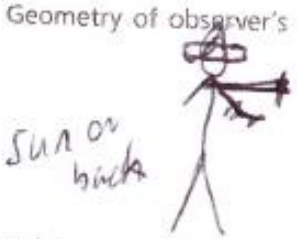

Height of instrument above ground 1.25 m Height of instrument above target

Scan No.	Target	Time	Sky Condition	Comments
4 Scans		1013	Clear	Lots of rocks
		1030		

COMMENTS: (Sketches may be helpful)

Instruction: This form provides for scans from several positions at each target, or scans from adjacent targets of the same type at the same site (e.g., same species of shrub). Use a separate form for each new site. Comments on individual scans could mention if a new reference scan was used, or if a sudden gust of wind arose. Comments for the site should mention nearby features that may affect overall incident radiation on the target, such as nearby trees, buildings, or landform features.